Front. Phys. 13(1), 130303 (2018)
DOI 10.1007/s11467-017-0709-3

RESEARCH ARTICLE

Cavity control as a new quantum algorithms implementation treatment

M. AbuGhanem[1,2,†], A. H. Homid[1,3], M. Abdel-Aty[1]

[1] *University of Science and Technology, Zewail City of Science and Technology, Giza, 12588, Egypt*
[2] *Department of Mathematics, Faculty of Science, Ain-Shams University, Cairo, 11566, Egypt*
[3] *Faculty of Science, Al-Azhar University, Assiut, 71524, Egypt*
Corresponding author. E-mail: [†] *gaa1nem@gmail.com*
Received March 17, 2017; accepted June 28, 2017

Based on recent experiments [*Nature* 449, 438 (2007) and *Nature Physics* 6, 777 (2010)], a new approach for realizing quantum gates for the design of quantum algorithms was developed. Accordingly, the operation times of such gates while functioning in algorithm applications depend on the number of photons present in their resonant cavities. Multi-qubit algorithms can be realized in systems in which the photon number is increased slightly over the qubit number. In addition, the time required for operation is considerably less than the dephasing and relaxation times of the systems. The contextual use of the photon number as a main control in the realization of any algorithm was demonstrated. The results indicate the possibility of a full integration into the realization of multi-qubit multiphoton states and its application in algorithm designs. Furthermore, this approach will lead to a successful implementation of these designs in future experiments.

Keywords quantum computation, quantum algorithms implementation, cavity control

PACS numbers 03.67.Lx, 03.67.Ac, 03.65.Ca

1 Introduction

Since World War II, researchers such as Alan Turing needed fast computation to decode encrypted messages. This was the reason that led Alan Turing to introduce the first mathematical notion of a programmable machine. Alan and Alonzo Church proposed a worldwide Turing machine that can be used to simulate any other Turing machine [1]. Ever since this development, conscientious efforts have been introduced to implement a quantum computer [2–6].

Scientists are still very assiduous in implementing a quantum computer, a machine that perform calculations depending on the laws of quantum mechanics, the most precise model of reality known at present. Quantum information and quantum computation are fields that have great significance for both theoretical and experimental studies in quantum mechanics [2] and have exhibited significant growth in recent years. Both fields have harnessed quantum physics to solve problems that have traditionally been approached using classical non-quantum ideas.

In the past few years, there has been a growing interest in both fields. These new approaches treat information and computation based on quantum theory and technology. Quantum information theory is based on physical information stored in the quantum state of a particular system. The development of quantum systems to store information has led to a deep understanding of the properties of enormous quantum systems.

This development aided in identifying physical systems from which a quantum computer can be implemented. The most convenient system that can execute a quantum algorithm is known as a nuclear magnetic resonance (NMR) quantum computer. There are also other systems such as neutral atoms, trapped ions, superconducting quantum interference devices (SQUIDs), nanoscale Josephson junctions and quantum dots [7–14].

Quantum technology as it develops offers hope for quantum devices to have enhanced computational speed and increased power to break unbreakable cryptosystems and offer enormous capabilities to solve hard problems with considerably less effort than its classical counterparts. Moreover, it introduces the possibility of having greater and more efficient information storage and re-

trieval systems. Recent studies indicate that computational devices can solve problems quicker than classical computers and can process information to preserve quantum coherence [15, 16].

A primary motivation for working in these fields is the prospect of developing fast quantum algorithms to solve complex computational problems and construct devices upon which such algorithms can be processed. In line with these goals, proposals for superconducting qubits are very promising. Recently, great progress has been made experimentally in the design of superconducting phase qubits. Moreover, Martinis [17] showed that the phase qubit has a potential advantage of scalability based on the low impedance of such devices and the microfabricability of complex structures. In addition, a detailed description was provided for the fabrication processes and the control electronics.

In addition to the demonstration in these systems of basic operations required for quantum computation, more complex algorithms are now within the reach of fabricable devices for potential applications. These facts have led to the consideration of superconducting phase qubits inductively coupled to a coplanar wave guide resonant cavity as a current model for study and for the development of algorithms. In recent years, theoretical and experimental modifications of quantum fluctuations of the -light emitted- in some physical systems were proved in Refs. [18–21].

This study demonstrates the characterization and realization of quantum algorithms defined in general multi-qubit systems. The extension of the Grover algorithm results in a general setting and may have several possible applications. The extended notion of cavity control to a multi-qubit setting involved a number of photons participating at different stages. Therefore, this significantly leads to risk exchanges at different times. Accordingly, the dissipation effect was ignored. For several years, significant efforts have been devoted to the study of dissipation [22]. One of the fundamental requirements for implementing a quantum computer known as DiVincenzo criteria [7] was that the physical system needed to have a long relevant decoherence time compared to that of the gate operation time.

This study presents a novel method for realizing one- and two-qubit gates to design quantum algorithms, such that the operation times of the quantum logic gates operating in algorithm applications depend on the number of photons present in their resonant cavities. Moreover, multi-qubit algorithms can be realized and the time required for operation is significantly less than the dephasing and relaxation times of the superconducting phase qubits.

In Section 2, this study briefly recall the main results on quantum algorithm optimality in a one-period setting. In Section 3, the key notions related to the implementation of quantum algorithms are extended to a general framework, involving preference functionals defined on a general quantum system. Section 4 demonstrates the necessary and sufficient experimental evidence and setting for experimental procedures with the required time to implement the gates. In Section 5, the results are illustrated using different relevant examples, where explicit characterizations of the transfer rule are obtained. Finally, the last section summarizes the results of this work and presents the conclusions.

2 Model

Understanding the basic theory of superconducting phase qubits that are inductively coupled to a coplanar waveguide resonant cavity is essential [12, 13]. These coupled systems are used to realize some of the useful gates that are applied in the implementation of quantum algorithms.

A phase qubit with n excess Cooper-pair charges consists of two superconducting islands that are connected to a superconducting electrode through two identical Josephson tunnel junctions E_J of a small size and having the same junction capacitance C_J. It is assumed that the qubit operates in a regime with $k_BT \ll E_C \ll E_J$, where $E_J = \hbar I_0/(2e)$, $E_C = 2e^2/C_J$, k_B, and T are the Josephson energy, the charging energy, the Boltzmann constant, and the temperature, respectively. If the Josephson junction is capacitively shunted and driven by a bias current I, the Hamiltonian of the qubit is given from Ref. [23] by $\hat{H}_{qu} = -E_C\frac{\partial^2}{\partial\Theta^2} - \frac{\hbar I}{2e}\Theta - E_J\cos\Theta$, where Θ and I_0 are the phase difference across the junction and the junction critical current, respectively.

When the junction bias current I is typically driven close to I_0, its parallel loop inductance produces a nonlinear potential, which is a function of Θ. The phase qubit is restricted to the two lowest energy states, the ground state $|g\rangle$ and the first excited state $|e\rangle$, where these states are encoded in the phase difference Θ across a large C_J. These states of the qubit resemble those of anharmonic LC oscillators. This study presented here is based on the experimental work of Simmonds *et al.* [24].

The model, based on the results offered in Refs. [25, 26], consisted of an open-ended coplanar waveguide cavity whose lowest standing wave eigenmode ($\lambda/2$ mode) is capacitively coupled to both ends of the two superconducting phase qubits, and where the qubits are connected via fixed coupling capacitors C_c (see Fig. 1 for a schematic). Each qubit state was read out individually in a single-shot manner by using an inductively coupled dc SQUID. This system is used throughout the following discussion to implement the quantum algorithms.

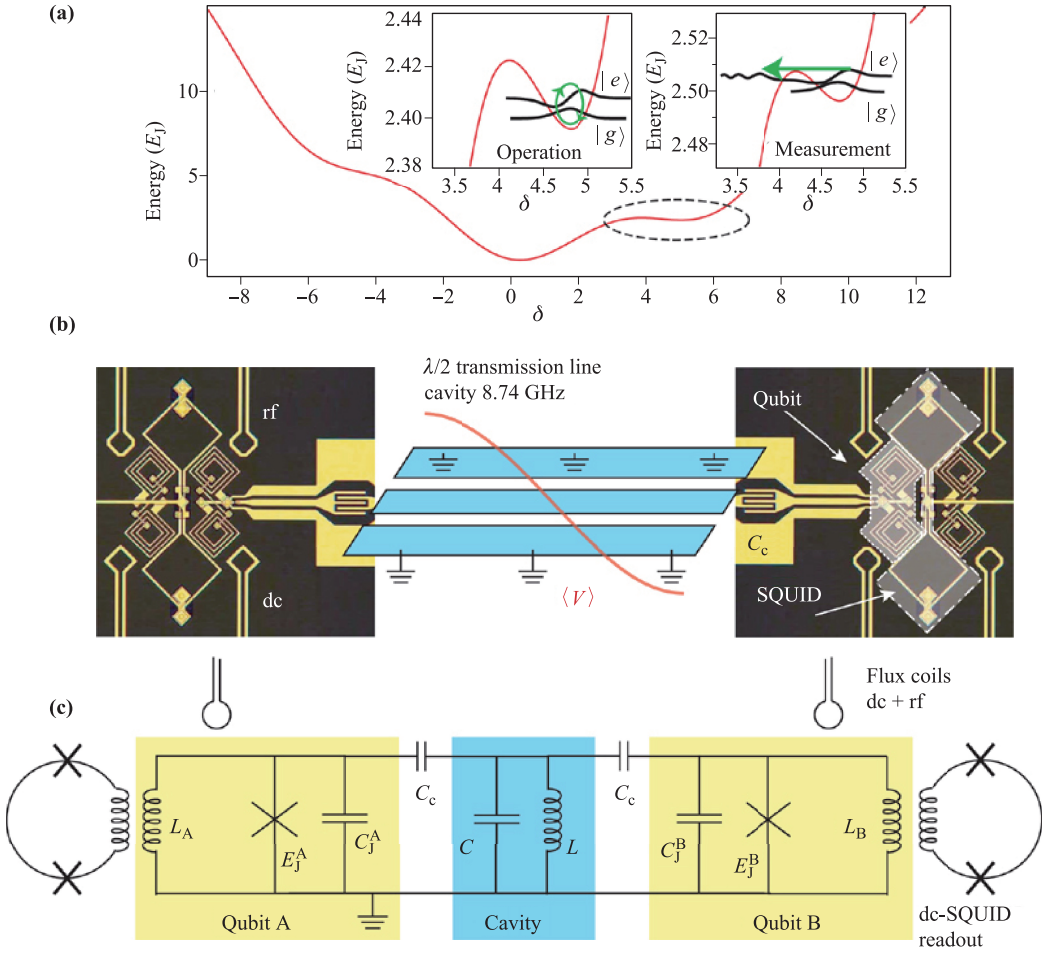

Fig. 1 Schematic description of the Sillanpää, Park, and Simmonds [25] experiment. **(a)** Potential energy diagram of the phase qubit (*red line*) and illustration of the operation and measurement (*green line*). The interaction circuit is composed of two Josephson phase qubits with a resonant cavity. **(b)** Illustration of the quantum memory element with two Josephson phase qubits connected via coupling capacitors to either end of a resonant cavity. **(c)** Lumped element equivalent circuit near the $\lambda/2$ resonance. Reprinted with permission from Ref. [25], Copyright 2007 © Nature Publishing Group.

The two phase qubits are inductively coupled to two separate flux bias coils. One set of these coils is used for adjusting a static dc-flux bias, and the other set of coils are rf-flux-biased. The coils enable rapid flux bias changes (shift pulses). In addition, the coils are used for single-shot state measurements and fast bias shifts. The coils allow the application of microwave pulses.

Throughout this work, every set of qubit dc-flux bias lines includes low-pass and copper powder filters, whereas the other set of rf-flux pulsed lines are combined into a single microwave coaxial line at room temperature and are attenuated by roughly 40 dB inside the cryostat.

Based on the experimental considerations introduced in Ref. [26], a rotating reference frame that rotates at an external driving field frequency ω_e was chosen. This choice changed the frequency of the cavity operator from ω_r to $\omega_r-\omega_e$. It also modified the frequency of the qubit operators from the frequencies $\omega_{A,B}$ to $\omega_{A,B}-\omega_e$. Under these considerations, the Hamiltonian of two flux-biased phase qubits coupled to a coplanar waveguide resonant cavity have the form

$$\hat{H} = \hbar\Delta_r\hat{a}^\dagger\hat{a} + \hbar\sum_{l=A,B}\Delta_l\hat{\sigma}_+^l\hat{\sigma}_-^l + \mathrm{i}\hbar\sum_{l=A,B}G_l\left(\hat{a}\hat{\sigma}_+^l - \mathrm{h.c.}\right), \quad (1)$$

where $\Delta_r=\omega_r-\omega_e$, $\Delta_l=\omega_l-\omega_e$, and $\hat{\sigma}_+^l(\hat{\sigma}_-^l)$ and $\hat{a}^\dagger(\hat{a})$ refer to the raising (lowering) operators of the qubits and cavity, respectively. In addition, in Eq. (1) $\omega_l=E_e^l-E_g^l$ are the qubit transition frequencies, ω_r is the cavity frequency, and $G_l=\frac{\omega_r C_c}{2\sqrt{CC_J^l}}$ are the effective coupling frequencies in which C_c is the capacitance of the coupling capacitors and C is the capacitance of the resonant cav-

ity. The qubit transition frequencies were controlled by the amplitude of the dc- and rf-flux bias. As a further restriction, the two superconducting phase qubits were assumed to be identical in the following treatments.

3 Realization of quantum gates

In the following study, the models are employed to realize one-qubit and two-qubit gates. For a one-qubit gate, it is assumed that the qubit B is kept off-resonance with respect to the resonant cavity mode. A time-dependent gauge transformation is then made on the system with the dynamical evolution generated by

$$\hat{u}_1(t) = \exp\left(\mathrm{i}\hbar t\Delta_r \hat{a}^\dagger\hat{a} + \mathrm{i}\hbar t\Delta_A \hat{\sigma}_+^A\hat{\sigma}_-^A + \mathrm{i}\phi_3\hat{\sigma}_+^A\hat{\sigma}_-^A\right).$$

By applying this transformation to the Hamiltonian in Eq. (1), the Hamiltonian in the new gauge becomes

$$\begin{aligned}\hat{H}_A(\phi_3) &= \hat{u}_1(t)\hat{H}\hat{u}_1^\dagger(t) - \mathrm{i}\hat{u}_1(t)\frac{\partial\hat{u}_1^\dagger(t)}{\partial t}\\ &= \mathrm{i}\hbar G_A\left(\hat{a}\hat{\sigma}_+^A\mathrm{e}^{\mathrm{i}\phi_3} - \mathrm{h.c.}\right).\end{aligned} \tag{2}$$

The Hamiltonian in Eq. (2), can be re-expressed in terms of an effective Hamiltonian that is diagonal. Accordingly, the phase variable ϕ_3 was modified to be complex and of the form $\phi_3 + \mathrm{i}\phi_4$. In terms of the new phase variable, the system in Eq. (2) was altered as follows:

$$\hat{H}_A(\phi_3,\phi_4) = \mathrm{i}\hbar G_A\left(\hat{a}\hat{\sigma}_+^A\mathrm{e}^{\mathrm{i}\phi_3}\mathrm{e}^{-\phi_4} - \hat{a}^\dagger\hat{\sigma}_-^A\mathrm{e}^{-\mathrm{i}\phi_3}\mathrm{e}^{\phi_4}\right). \tag{3}$$

The value of parameter ϕ_4 was set to be $\frac{2}{\hbar^2\omega_A}$ and the system was considered for configurations satisfying the condition $\frac{G_A}{\omega_A} \ll 1$. The effective Hamiltonian then took the form

$$\begin{aligned}&\hat{H}_A(\phi_3)\\ &= \hat{H}_A\left(-\phi_3, \frac{2}{\hbar^2\omega_A}\right)\times\hat{H}_A\left(\phi_3, -\frac{2}{\hbar^2\omega_A}\right)\\ &= \frac{4G_A^2}{\omega_A}\left[\hat{a}^\dagger\hat{a}(2\mathrm{i}\hat{\sigma}_+^A\hat{\sigma}_-^A\sin(2\phi_3) - \hat{\sigma}_z^A\mathrm{e}^{2\mathrm{i}\phi_3}) - \hat{\sigma}_+^A\hat{\sigma}_-^A\mathrm{e}^{-2\mathrm{i}\phi_3}\right].\end{aligned} \tag{4}$$

The time evolution of the system in Eq. (4) can be described by the diagonal Hamiltonian as follows:

$$\hat{U}_A(\phi_3,t_1) = \mathrm{e}^{\mathrm{i}\xi_A t_1}|e_A,r\rangle\langle e_A,r| + \mathrm{e}^{\mathrm{i}\xi'_A t_1}|g_A,r\rangle\langle g_A,r|, \tag{5}$$

where $\xi_A = \frac{4G_A^2}{\hbar\omega_A}[r\mathrm{e}^{2\mathrm{i}\phi_3} + \mathrm{e}^{-2\mathrm{i}\phi_3} - 2\mathrm{i}r\sin(2\phi_3)]$ and $\xi'_A = -\frac{4rG_A^2}{\hbar\omega_A}\mathrm{e}^{2\mathrm{i}\phi_3}$. If $\phi_3 = \pi$, it follows from Eq. (5) that

$$\mathrm{e}^{-\mathrm{i}\xi_2^A t_1}\hat{U}_A(\pi,t_1) = \mathrm{e}^{\mathrm{i}(\xi_1^A-\xi_2^A)t_1}|e_A,r\rangle\langle e_A,r| + |g_A,r\rangle\langle g_A,r| \tag{6}$$

and

$$\mathrm{e}^{-\mathrm{i}\xi_1^A t_1}\hat{U}_A(\pi,t_1) = |e_A,r\rangle\langle e_A,r| + \mathrm{e}^{-\mathrm{i}(\xi_1^A-\xi_2^A)t_1}|g_A,r\rangle\langle g_A,r|, \tag{7}$$

where $\xi_1^A = \frac{4G_A^2}{\hbar\omega_A}(r+1)$ and $\xi_2^A = -\frac{4rG_A^2}{\hbar\omega_A}$. Recently, a more rigorous derivation of effective Hamiltonian theory and its domain of applicability and a developed technique for finding the dynamical evolution in time of an averaged density matrix were discussed [27]. Following the action of a π pulse ($\chi_A t_1 = \pi$ where $\chi_A = G_A^2(2r+1)$), the one-qubit phase gates and the elementary rotation gate about the z axis can be realized from Eqs. (6) and (7) as follows:

$$\mathrm{S}_e^A(\Phi) = \mathrm{e}^{\frac{\mathrm{i}\Phi}{2}}|e_A,r\rangle\langle e_A,r| + |g_A,r\rangle\langle g_A,r|, \tag{8}$$

$$\mathrm{S}_g^A(\Phi) = |e_A,r\rangle\langle e_A,r| + \mathrm{e}^{\frac{-\mathrm{i}\Phi}{2}}|g_A,r\rangle\langle g_A,r|, \tag{9}$$

$$\mathrm{R}_z^A(\Phi) = \mathrm{S}_e^A(\Phi)\mathrm{S}_g^A(\Phi), \text{ with } \Phi = \frac{8\pi}{\hbar\omega_A}. \tag{10}$$

In addition, by using the canonical transformation $\hat{F} = \exp(\frac{\mathrm{i}\pi}{4}\hat{\sigma}_y^A)$ on the system in Eq. (4), it follows that

$$\hat{H}'_A = \hat{F}\,\hat{H}_A(\pi)\hat{F}^\dagger = \frac{2G_A^2}{\omega_A}\left[(2\hat{a}^\dagger\hat{a}+1)\hat{\sigma}_x^A - \hat{\mathbb{I}}\right] \tag{11}$$

generates a realization of the other one-qubit gates. The dynamical evolution of the system in Eq. (11) can then be expressed as follows:

$$\begin{aligned}\hat{V}_A(t_1) = \mathrm{e}^{\mathrm{i}\upsilon_1 t_1}\Big[&\cos(\upsilon_2 t_1)(|e_A,r\rangle\langle e_A,r| + |g_A,r\rangle\langle g_A,r|)\\ &-\mathrm{i}\sin(\upsilon_2 t_1)(|e_A,r\rangle\langle g_A,r| + |g_A,r\rangle\langle e_A,r|)\Big],\end{aligned} \tag{12}$$

where $\upsilon_1 = \frac{2G_A^2}{\hbar\omega_A}$ and $\upsilon_2 = \frac{2G_A^2}{\hbar\omega_A}(2r+1)$.

In the following context, a realization was made about the elementary rotation gates about the x and y axes, the NOT gate (NOT^A) and the Hadamard gate (H^A). This is done, respectively, by the following associations:

- $\exp(\frac{-2\mathrm{i}\pi\upsilon_1}{\chi_A})\hat{V}_A(\frac{2\pi}{\chi_A}) \to \mathrm{R}_x^A(\Phi)$,
- $\mathrm{S}_g^A(\pi)\mathrm{R}_x^A(\Phi)(\mathrm{S}_g^A(\pi))^{-1} \to \mathrm{R}_y^A(\Phi)$,
- $\mathrm{S}_e^A(2\pi)\mathrm{R}_x^A(\pi)\mathrm{R}_z^A(\pi) \to \mathrm{NOT}^A$,
- $\mathrm{e}^{\frac{\mathrm{i}\pi}{2}}\mathrm{R}_z^A(\frac{\pi}{2})\mathrm{R}_x^A(\frac{\pi}{2})\mathrm{R}_z^A(\frac{\pi}{2}) \to \mathrm{H}^A$.

In the same manner, if the qubit A was kept off-resonance with respect to the cavity mode, the dynamical evolution operators $\hat{U}_B(\phi_3,t_1)$ and $\hat{V}_B(t_1)$ can be introduced. In terms of these new B variable operators, the above gates can be written as B qubit gates. Consideration was next given to two-qubit gates.

To realize a two-qubit gate, a time-dependent gauge transformation associated with the dynamical evolution developed by

$$\hat{u}_2(t) = \prod_{l=A,B}\exp\left(\mathrm{i}\hbar t\Delta_r\hat{a}^\dagger\hat{a} + \mathrm{i}\hbar t\Delta_l\hat{\sigma}_+^l\hat{\sigma}_-^l + \mathrm{i}(\phi_1-\phi_2)\hat{a}^\dagger\hat{a}\right)$$

was introduced. By applying this transformation, the Hamiltonian of Eq. (1) in the new gauge becomes

$$\hat{H}(\phi_1,\phi_2)=\hat{u}_2(t)\hat{H}\hat{u}_2^{\dagger}(t)-\mathrm{i}\hat{u}_2(t)\frac{\partial\hat{u}_2^{\dagger}(t)}{\partial t}$$
$$=\mathrm{i}\hbar\sum_{l=A,B}G_l\Big[\hat{a}\hat{\sigma}_+^l\mathrm{e}^{-\mathrm{i}(\phi_1-\phi_2)}-\hat{a}^{\dagger}\hat{\sigma}_-^l\mathrm{e}^{\mathrm{i}(\phi_1-\phi_2)}\Big]. \tag{13}$$

For the sake of simplicity, we apply the canonical transformation $\hat{\Upsilon}_1=\exp(-\frac{\mathrm{i}\pi}{4}(\hat{\sigma}_x^A+\hat{\sigma}_x^B))$ on the Hamiltonian of Eq. (13). From the application of this transformation, we obtain the transformed Hamiltonian

$$\hat{H}_1(\phi_1,\phi_2)=\hat{\Upsilon}_1\hat{H}(\phi_1,\phi_2)\hat{\Upsilon}_1^{\dagger}$$
$$=\hbar\sum_{l=A,B}\frac{G_l}{2}\Big\{-[\hat{a}\mathrm{e}^{-\mathrm{i}(\phi_1-\phi_2)}+\mathrm{h.c.}]\hat{\sigma}_z^l$$
$$+\mathrm{i}[\hat{a}\mathrm{e}^{-\mathrm{i}(\phi_1-\phi_2)}-\mathrm{h.c.}]\hat{\sigma}_x^l\Big\}. \tag{14}$$

This was followed by making a time-I gauge transformation of the resulting Hamiltonian, which was given by $\hat{\Upsilon}_2=\exp\big(-\mathrm{i}\hbar\omega_r(\hat{\sigma}_z^A+\hat{\sigma}_z^B)\big)$. The Hamiltonian of Eq. (14) in the new gauge then becomes

$$\hat{H}_2(\phi_1,\phi_2)=\hat{\Upsilon}_2\hat{H}_1(\phi_1,\phi_2)\hat{\Upsilon}_2^{\dagger}$$
$$=\hbar\sum_{l=A,B}\frac{G_l}{2}\Big\{-[\hat{a}\mathrm{e}^{-\mathrm{i}(\phi_1-\phi_2)}+\mathrm{h.c.}]\hat{\sigma}_z^l$$
$$+\mathrm{i}[\hat{a}\mathrm{e}^{-\mathrm{i}(\phi_1-\phi_2)}-\mathrm{h.c.}](\hat{\sigma}_+^l\mathrm{e}^{-2\mathrm{i}\hbar\omega_r}+\mathrm{h.c.})\Big\}. \tag{15}$$

Under the condition $\frac{G_l}{2}\ll\omega_l$ and ω_r, the rotating wave approximation was applied, where $\pm2\omega_r=\pm(\omega_r+\omega_r)=\pm(\omega_l+\omega_r)$, in which very fast oscillating terms were neglected. By setting the parameter ϕ_1 equal to $\frac{2}{\hbar^2\omega_l}$, and from the above condition that $G_l\ll\omega_l$, the following equation was obtained:

$$\hat{H}_3(\phi_2)=\hat{H}_2\left(\frac{2}{\hbar^2\omega_l},-\phi_2\right)\times\hat{H}_2\left(-\frac{2}{\hbar^2\omega_j},\phi_2\right)$$
$$=-\frac{2\hat{a}\hat{a}^{\dagger}\sin(2\phi_2)+\mathrm{ie}^{2\mathrm{i}\phi_2}}{2}$$
$$\cdot\sum_{l,j=A,B}\frac{G_lG_j(\omega_l+\omega_j)}{\omega_l\omega_j}\hat{\sigma}_z^l\hat{\sigma}_z^j. \tag{16}$$

The dynamical evolution of the system in Eq. (16) at $\phi_2=\pi/4$ is given by the following evolution operator:

$$\hat{U}(t_2)=\mathrm{e}^{\mathrm{i}\alpha t_2}|e_A,e_B,r\rangle\langle e_A,e_B,r|+|e_A,g_B,r\rangle\langle e_A,g_B,r|$$
$$+|g_A,e_B,r\rangle\langle g_A,e_B,r|+\mathrm{e}^{\mathrm{i}\alpha t_2}|g_A,g_B,r\rangle\langle g_A,g_B,r|, \tag{17}$$

where $\alpha=\frac{\chi_A\Phi}{2\pi}$. Following the action of a π pulse ($\chi_At_2=\pi$), the dynamical evolution from Eq. (17) proceeds as follows: The π pulse first acts on the system with the unitary operator $\hat{U}\big(\frac{\pi}{\chi_A}\big)$ and then the transformation $R_1=R_x^A(\pi)\otimes R_x^B(2\pi)$ is applied on the unitary operator. Consequently, the two-qubit conditional phase gates labeling different target states were realized by the following sets of operations:

- $\big(S_e^A(\Phi)\otimes S_g^B(\Phi)\big)\hat{U}\big(\frac{\pi}{\chi_A}\big)\rightarrow\mathrm{P}_{ee}(\Phi)$,
- $\big(S_e^A(\Phi)\otimes S_g^B(\Phi)\big)^{-1}\hat{U}\big(\frac{\pi}{\chi_A}\big)\rightarrow\mathrm{P}_{gg}(\Phi)$,
- $R_1\mathrm{P}_{ee}(\Phi)R_1^{\dagger}\rightarrow\mathrm{P}_{ge}(\Phi)$,
- $R_1\mathrm{P}_{gg}(\Phi)R_1^{\dagger}\rightarrow\mathrm{P}_{eg}(\Phi)$.

Apart from these gates, two-qubit controlled NOT (CNOT) gates were realized in the following context. If qubit A was the control qubit and qubit B was the target qubit, the controlled NOT gate was represented by CNOT, whereas if qubit B was the control qubit and qubit A was the target qubit, the controlled NOT gate was represented by CNOT_1. By evaluating

$$R_2\mathrm{P}_{ee}(\Phi)R_2=\frac{\mathrm{e}^{\mathrm{i}\Phi}+1}{2}\Big(|e_A,e_B,r\rangle\langle e_A,e_B,r|+|e_A,g_B,r\rangle\langle e_A,g_B,r|\Big)$$
$$+\frac{-\mathrm{e}^{\mathrm{i}\Phi}+1}{2}\Big(|e_A,e_B,r\rangle\langle e_A,g_B,r|+|e_A,g_B,r\rangle\langle e_A,e_B,r|\Big)$$
$$+|g_A,e_B,r\rangle\langle g_A,e_B,r|+|g_A,g_B,r\rangle\langle g_A,g_B,r|, \tag{18}$$
$$R_3\mathrm{P}_{ee}(\Phi)R_3=\frac{\mathrm{e}^{\mathrm{i}\Phi}+1}{2}\Big(|e_A,e_B,r\rangle\langle e_A,e_B,r|+|g_A,e_B,r\rangle\langle g_A,e_B,r|\Big)$$
$$+\frac{-\mathrm{e}^{\mathrm{i}\Phi}+1}{2}\Big(|g_A,e_B,r\rangle\langle e_A,e_B,r|+|e_A,e_B,r\rangle\langle g_A,e_B,r|\Big)$$
$$+|e_A,g_B,r\rangle\langle e_A,g_B,r|+|g_A,g_B,r\rangle\langle g_A,g_B,r|, \tag{19}$$

where $R_2=\mathrm{R}_x^A(4\pi)\otimes\mathrm{H}^B$ and $R_3=\mathrm{H}^A\otimes\mathrm{R}_x^B(4\pi)$, the representation of the two different controlled NOT gates becomes $R_2\mathrm{P}_{ee}(\pi)R_2\rightarrow\mathrm{CNOT}$ and $R_3\mathrm{P}_{ee}(\pi)R_3\rightarrow\mathrm{CNOT}_1$.

Additionally, to realize another set of two-qubit gates, the above system in Eq. (13) and the condition $G_l \ll \omega_l$ were considered. In this limit, the following was obtained:

$$\begin{aligned}\hat{H}_Q &= \hat{H}\left(-\frac{2}{\hbar^2\omega_l}, \frac{3\pi}{4}\right) \times \hat{H}\left(\frac{2}{\hbar^2\omega_j}, -\frac{3\pi}{4}\right) \\ &= \frac{4G_1^2}{\omega_1}\Big[(2\hat{a}^\dagger\hat{a}+1)(\hat{\sigma}_+^1\hat{\sigma}_-^2 + \hat{\sigma}_+^2\hat{\sigma}_-^1) \\ &\quad +2\hat{a}^\dagger\hat{a} + \hat{\sigma}_+^1\hat{\sigma}_-^1 + \hat{\sigma}_+^2\hat{\sigma}_-^2\Big], \end{aligned} \tag{20}$$

where $1 \equiv A$ and $2 \equiv B$. To this Hamiltonian a time-dependent gauge transformation given by the unitary operator

$$\hat{u}_3(t) = \prod_{l=A,B} \exp\left(-\mathrm{i}\frac{4G_A^2}{\omega_A}\left(2\hat{a}^\dagger\hat{a} + \hat{\sigma}_+^l\hat{\sigma}_-^l\right)t\right)$$

was applied. Under this transformation, the Hamiltonian in (20) within the new gauge became

$$\hat{H}'_Q = \hat{u}_3^\dagger(t)\hat{H}_Q\hat{u}_3(t) - \mathrm{i}\hat{u}_3^\dagger(t)\frac{\partial\hat{u}_3(t)}{\partial t}. \tag{21}$$

The time evolution of the system in Eq. (21) was then given by

$$\begin{aligned}\hat{U}_Q(t_2) &= |e_A,e_B,r\rangle\langle e_A,e_B,r| - \mathrm{i}\sin(\alpha t)\{|e_A,g_B,r\rangle\langle g_A,e_B,r| + |g_A,e_B,r\rangle\langle e_A,g_B,r|\} \\ &\quad +\cos(\alpha t)\{|e_A,g_B,r\rangle\langle e_A,g_B,r| + |g_A,e_B,r\rangle\langle g_A,e_B,r|\} + |g_A,g_B,r\rangle\langle g_A,g_B,r|. \end{aligned} \tag{22}$$

Following the action of a $\pi/2$ pulse ($\alpha t_2 = \pi/2$), the following two-qubit gates were realized:

- $\hat{U}_Q\left(\frac{\pi}{2\alpha}\right) \to -$iSWAP-gate,
- $R_1^\dagger\hat{U}\left(\frac{\pi}{2\alpha}\right)R_1\hat{U}_Q\left(\frac{\pi}{2\alpha}\right) \to$ SWAP-gate.

Moreover, the following new set of two-qubit gates were obtained:

- $[S_e^A(\pi)\otimes S_e^B(\pi)]^{-1}\hat{U}_Q\left(\frac{\pi}{2\alpha}\right) \to -$SWCZ-gate,
- $\mathrm{P}_{ee}(\Phi) \times \mathrm{SWAP} \to \mathrm{CR}_k\mathrm{S}$-gate, $k = \log_2\left(\frac{2\pi}{\Phi}\right)$,
- $[S_e^A(\frac{\pi}{2})\otimes S_e^B(\frac{\pi}{2})]^{-1}\hat{U}_Q\left(\frac{\pi}{4\alpha}\right) \to \mathrm{i}\sqrt{\mathrm{SWCZ}}$-gate.

Based on the new techniques developed earlier to realize the above gates, quantum algorithms can be implemented as previously studied in other formats.

4 Implementation of quantum algorithms

Quantum algorithms are procedures for performing computations in quantum systems. They are implementable as quantum circuits involving the components of the quantum systems studied. The realization of quantum algorithms, in general, is made through the implementation of a finite number of logical gates, which are sequentially activated within the quantum system. In this study, the emphasis is on the most commonly used algorithms in the formulations that are constructed.

The most commonly used algorithm is the discrete quantum Fourier transform (DQFT) algorithm [28–32]. Other algorithms, such as the quantum search algorithm for searching an unstructured database [33] and the Deutsch–Jozsa algorithm for solving a black-box problem [34] are also commonly used. One should also note that the DQFT belongs to a bigger class of quantum algorithms. The most notable examples are Simon's algorithm [35, 36], the phase estimation algorithm for estimating the eigenphase of an eigenvector of a unitary gate [28, 37], and Shor's factoring algorithm [38, 39].

Areas in which quantum algorithms are applicable include quantum cryptography, information search, annealing, and the solution of large systems of linear equations. In the development of N-qubit algorithms, the design of one- and two-qubit gates is an important initial step. In this study, we focus on the types of gates required to realize N-qubit algorithms and numerical results of the time necessary for the operation of some of these algorithms. In addition, we develop new ideas for future experimental realization of these algorithms and discuss results concerning the influence of photon number on their required operation time. Numerous methods and techniques have been developed to get an exact or even an approximate solution of the Schrödinger equation, including perturbation theory, variational methods, diagram methods, and the JWBK approximation method [40–42]. New analytical methods to solve the Schrödinger equation were introduced in Ref. [43].

Some interesting quantum algorithms can be implemented as follows:

- Using H^l, $\mathrm{P}_{ee}(\Phi)$, and SWAP gates at different Φ, the basic DQFT that was realized in Ref. [28] can be realized.
- Using H^l, $\mathrm{R}_z^l(\Phi)$, $\mathrm{S}^l(\Phi)$, CNOT_1, and $-$SWCZ gates at different Φ, one can implement the DQFT that was realized in Ref. [29].
- Using H^A and $\mathrm{CR}_k\mathrm{S}$ gates, one can realize the DQFT that was realized in Ref. [30].
- Using H^A, $\mathrm{R}_x^l(\Phi)$, $\mathrm{R}_y^l(\Phi)$, $\mathrm{R}_z^l(\Phi)$, and $-$iSWAP

gates at different Φ, one can implement the DQFT the was realized in Ref. [31].

- Using H^l, $R_z^l(\Phi)$, $S^l(\Phi)$, $P_{ee}(\Phi)$, and $i\sqrt{SWCZ}$ gates at different Φ, one can implement the DQFT that was realized in Ref. [32].
- Using H^l and the controlled phase gates for the label different target states, one can implement the two-qubit quantum search algorithm mentioned in Ref. [33].
- Using H^l and CNOT gates, one can implement the Deutsch–Jozsa algorithm, such as that mentioned in Ref. [34].
- Using H^l, NOT^l, and CNOT gates, one can implement the quantum Simon's algorithm that was realized in Refs. [35, 36].
- Using H^l, controlled phase gates, and the inverse of one of the DQFT algorithms above, one can implement the phase estimation algorithm that was realized in Refs. [28, 37].
- Using H^l, CNOT, and $CNOT_1$ gates and the inverse of one of the DQFT algorithms above, one can implement the quantum Shor's algorithm that was realized in Refs. [38, 39].

5 Experimental evidence and discussion

In this section, we assume that the devices under consideration are fabricated by means of standard optical lithography with $Al/AlO_x/Al$ junctions on a sapphire substrate (see Refs. [25, 26]). In addition, the insulator between the metallic layers is SiO_2. The available data from these experiments are used to discuss the required times to implement the gates. For the aforementioned experiments, the parameters used were as follows: $C_c \simeq 6.38$ fF, $C \simeq 0.57$ pF, effective inductance of the cavity $L \simeq 560$ pH, inductance of the qubits $L_{A,B} \simeq 690$ nH, $E_J^{A,B} \simeq 45$ K, $C_J^{A,B} \simeq 0.7$ pF, the length of the coplanar waveguide resonant cavity was ~7 mm, and the junction areas were ~6 μm^2.

Based on these values, then it follows that $\frac{w_r}{2\pi} = \frac{1}{2\pi\sqrt{LC}} \simeq 8.9$ GHz and $G_{A,B} = \frac{\omega_r C_c}{2\sqrt{CC_J^{A,B}}} \simeq 90\pi$ MHz. As showed by You and Nori [44], in all previous experimental work on superconducting phase qubits performed to calculate the dephasing time (T_1) and relaxation time (T_2), the range of values ($T_1 = 0.1$–1 μs) and ($T_2 = 1$–10 μs) should represent the operation of these gates.

The objective of this study is to demonstrate that the required times for running the quantum gates to implement the quantum algorithms depend on the number of photons (r) in the cavity. The calculations were performed and the results in Table 1 display the required times to realize one-qubit gates and two-qubit gates. In Table 1 the times required for operating the one-qubit gates and some of the two-qubit gates are measured in attosecond units. Owing to the very small nature of these times, they have little effect on the system when they are added to the times required for implementing the two-qubit gates; for instance, the time of operation of the SWAP-gate is approximately the same as the time of operation of the CR_kS-gate, etc. Note that when r is increased, the times required for realizing the quantum gates are accordingly decreased. Consequently, the more r is increased, the greater is the correspondingly decrease

Table 1 Required times of the experimental feasibility for realizing one- and two-qubit quantum gates, where $l = A\&B$.

Gates	Required times										
	$r=0$	$r=1$	$r=2$	$r=3$	$r=4$	$r=5$	$r=6$	$r=7$	$r=8$	$r=9$	$r=10$
$S_e^l\&S_g^l$	39.30 as	13.11 as	7.860 as	5.614 as	4.366 as	3.573 as	3.023 as	2.620 as	2.312 as	2.068 as	1.871 as
$R_x^l\&R_z^l$	78.60 as	26.22 as	15.72 as	11.23 as	8.732 as	7.145 as	6.046 as	5.240 as	4.624 as	4.136 as	3.742 as
R_y^l	157.2 as	52.44 as	31.44 as	22.45 as	17.46 as	14.29 as	12.09 as	10.48 as	9.248 as	8.272 as	7.484 as
NOT^l	196.5 as	65.50 as	39.30 as	28.07 as	21.83 as	17.86 as	15.11 as	13.11 as	11.56 as	10.34 as	9.357 as
H^l	235.8 as	78.61 as	47.16 as	33.68 as	26.20 as	21.43 as	18.14 as	15.72 as	13.87 as	12.41 as	11.23 as
$P_{ee}\&P_{gg}$	117.9 as	39.33 as	23.58 as	16.84 as	13.11 as	10.72 as	9.069 as	7.859 as	6.936 as	6.204 as	5.613 as
$P_{eg}\&P_{ge}$	432.3 as	144.1 as	86.45 as	61.75 as	48.03 as	39.30 as	33.25 as	28.82 as	25.43 as	22.75 as	20.58 as
$CNOT\&CNOT_1$	746.7 as	249.1 as	149.3 as	106.7 as	82.96 as	67.88 as	57.43 as	49.78 as	43.92 as	39.30 as	35.55 as
SWAP	549.4 ns	183.1 ns	109.9 ns	78.48 ns	61.04 ns	49.94 ns	42.26 ns	36.63 ns	32.32 ns	28.92 ns	26.16 ns
−iSWAP	274.7 ns	91.56 ns	54.94 ns	39.24 ns	30.52 ns	24.97 ns	21.13 ns	18.31 ns	16.16 ns	14.46 ns	13.08 ns
−SWCZ	274.7 ns	91.56 ns	54.94 ns	39.24 ns	30.52 ns	24.98 ns	21.14 ns	18.31 ns	16.16 ns	14.46 ns	13.08 ns
$i\sqrt{SWCZ}$	137.4 ns	45.78 ns	27.47 ns	19.62 ns	15.26 ns	12.49 ns	10.57 ns	9.156 ns	8.079 ns	7.229 ns	6.540 ns
CR_kS	549.38 ns	183.13 ns	109.88 ns	78.483 ns	61.043 ns	49.944 ns	42.260 ns	36.626 ns	32.317 ns	28.915 ns	26.161 ns

in implementation times of quantum algorithms involving N qubits.

However, algorithms mentioned in Refs. [28–32] required one-qubit gates in addition to the two-qubit gates in their realization. If the number of one-qubit auxiliary gates in the algorithm realization reaches thousands of gates, the operation times of these gates may have some effect when added to the times of the two-qubit gates. For example, if an algorithm requires 6 two-qubit gates and 600 one-qubit gates and another algorithm requires 20 two-qubit gates and 2000 one-qubit gates, the total time for implementing these two different algorithm is essentially the time of the two-qubit gates. Hence, the total time taken to complete the procedure of these algorithms is the same as that of the two- qubit gates as listed in Tables 2–4.

As mentioned earlier, Tables 2 and 3 indicate that the time required for implementing algorithms in Refs. [28, 29] agree with the times in Refs. [30, 32]. Consequently, owing to the shortness of one-qubit gates time, the total time for three-qubit and four-qubit algorithms in Refs. [29, 32] are identical to the total time for two-qubit and three-qubit algorithms mentioned in Ref. [31], respectively.

The first row of the algorithm in Ref. [33] represents the times of the algorithm when the state searched for is $|ee\rangle$ or $|gg\rangle$. The second row represents the times of the algorithm when the state searched for is $|eg\rangle$ or $|ge\rangle$. In addition, Table 4 shows the basic circuit of the algorithm presented in Ref. [34], in which a one-qubit version of the Deutsch–Jozsa algorithm using the two-qubit states in the cavity is implemented. More importantly, the required times of the algorithms in Refs. [33, 34] are much less than T_1 and T_2. Consequently, the implementation of the algorithms in Refs. [33, 34] via our proposed system of study is a very effective method and is more

Table 2 Required times of the experimental feasibility for implementing previous two-qubit DQFT algorithms, where M. A. refer to the mentioned algorithm.

Algorithms	Required times of algorithms										
	$r=0$	$r=1$	$r=2$	$r=3$	$r=4$	$r=5$	$r=6$	$r=7$	$r=8$	$r=9$	$r=10$
M. A. in [28]	549.38 ns	183.13 ns	109.88 ns	78.483 ns	61.043 ns	49.944 ns	42.260 ns	36.626 ns	32.317 ns	28.915 ns	26.161 ns
M. A. in [29]	274.69 ns	91.564 ns	54.938 ns	39.242 ns	30.521 ns	24.972 ns	21.130 ns	18.313 ns	16.158 ns	14.457 ns	13.081 ns
M. A. in [30]	549.38 ns	183.13 ns	109.88 ns	78.483 ns	61.043 ns	49.944 ns	42.260 ns	36.626 ns	32.317 ns	28.915 ns	26.161 ns
M. A. in [31]	824.07 ns	274.69 ns	164.81 ns	117.72 ns	91.564 ns	74.916 ns	63.390 ns	54.938 ns	48.475 ns	43.372 ns	39.242 ns
M. A. in [32]	274.69 ns	91.564 ns	54.938 ns	39.242 ns	30.521 ns	24.972 ns	21.130 ns	18.313 ns	16.158 ns	14.457 ns	13.081 ns

Table 3 Required times of the experimental feasibility for implementing previous three-qubit DQFT algorithms.

Algorithms	Required times of algorithms										
	$r=0$	$r=1$	$r=2$	$r=3$	$r=4$	$r=5$	$r=6$	$r=7$	$r=8$	$r=9$	$r=10$
M. A. in [28]	1.6481 μs	549.38 ns	329.63 ns	235.45 ns	183.13 ns	149.83 ns	126.78 ns	109.88 ns	96.950 ns	86.745 ns	78.483 ns
M. A. in [29]	824.07 ns	274.69 ns	164.81 ns	117.72 ns	91.564 ns	74.916 ns	63.390 ns	54.938 ns	48.475 ns	43.372 ns	39.242 ns
M. A. in [30]	1.6481 μs	549.38 ns	329.63 ns	235.45 ns	183.13 ns	149.83 ns	126.78 ns	109.88 ns	96.950 ns	86.745 ns	78.483 ns
M. A. in [31]	2.4722 μs	824.07 ns	494.44 ns	353.17 ns	274.69 ns	224.75 ns	190.17 ns	164.81 ns	145.42 ns	130.12 ns	117.72 ns
M. A. in [32]	824.07 ns	274.69 ns	164.81 ns	117.72 ns	91.564 ns	74.916 ns	63.390 ns	54.938 ns	48.475 ns	43.372 ns	39.242 ns

Table 4 Required times of the experimental feasibility for implementing quantum search and quantum Deutsch–Jozsa algorithms, respectively.

Algorithms	Required times of algorithms										
	$r=0$	$r=1$	$r=2$	$r=3$	$r=4$	$r=5$	$r=6$	$r=7$	$r=8$	$r=9$	$r=10$
M. A. in [33]	1.6505 fs	0.55017 fs	0.33010 fs	0.23579 fs	0.18339 fs	0.15005 fs	0.12696 fs	0.11003 fs	0.09709 fs	0.08687 fs	0.07860 fs
	1.9649 fs	0.65496 fs	0.39298 fs	0.28070 fs	0.21832 fs	0.17863 fs	0.15114 fs	0.13099 fs	0.11558 fs	0.10341 fs	0.09357 fs
M. A. in [34]	3.3010 fs	1.1003 fs	0.66020 fs	0.47157 fs	0.36678 fs	0.30009 fs	0.25392 fs	0.22007 fs	0.19418 fs	0.17374 fs	0.15719 fs

effective than that used in other systems.

Figures 2 and 3 show the effects of photon number on the implementation times required for the algorithms in Refs. [28–34] for systems containing up to 40 and up to 2000 photons. This comparison focuses on determining the influence of photon number on the implementation times for systems composed of algorithms of a few qubits and for systems composed of algorithms with many qubits, respectively.

In the absence of photons in the cavity, the two-qubit algorithms described in Refs. [28–32] can be implemented experimentally. This is because the required times for implementing these algorithms are less than T_1 and T_2 [see the bottom curves in Figs. 2(a)–(e) and Tables 2 and 3]. Furthermore, the three-qubit algorithms presented in Refs. [29, 32] can be realized, whereas the four-qubit

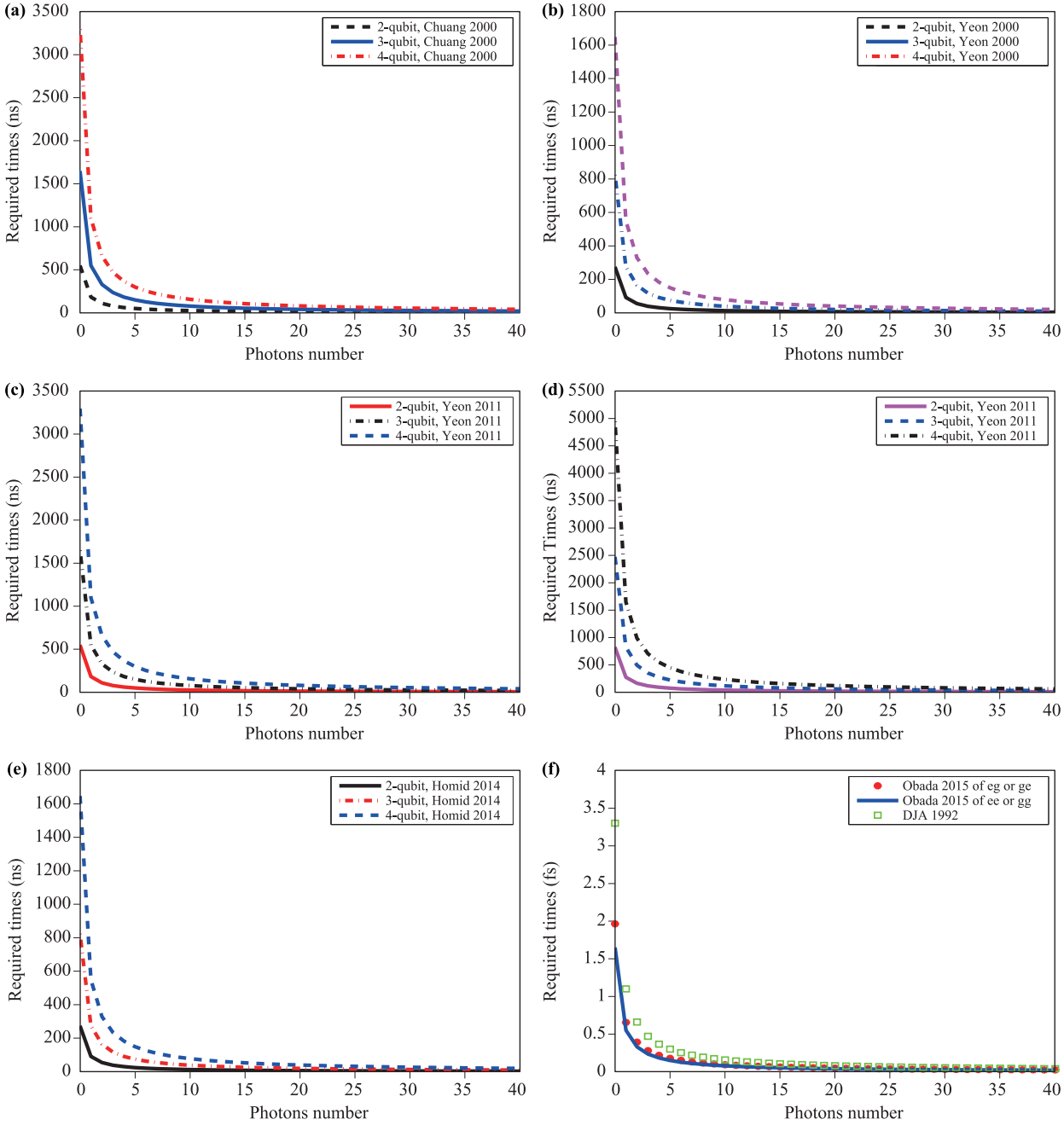

Fig. 2 Required times versus photon number for two-, three-, and four-qubit algorithms in the case of resonance, where **(a)** M. A. in [28], **(b)** M. A. in [29], **(c)** M. A. in [30], **(d)** M. A. in [31], **(e)** M. A. in [32], and **(f)** M. A. in [33, 34].

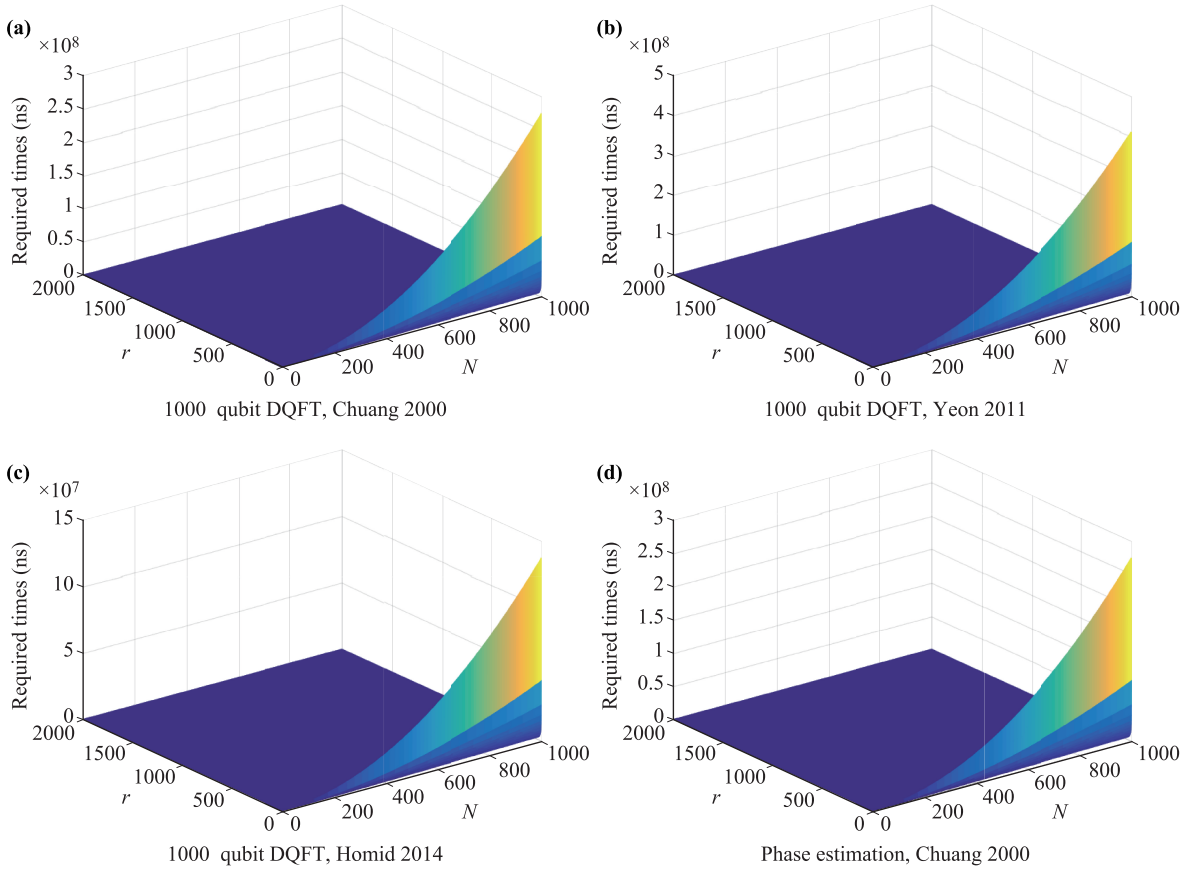

Fig. 3 Required times for some algorithms versus qubit number and photon number in the case of resonance, where N ranges from 2 to 1000.

versions of these algorithms cannot. This is because the implementation times of the algorithms are longer than their dephasing times [see the middle and the top curves in Figs. 2(b) and (e)].

The reason why the three- and four-qubit algorithms in Refs. [28, 30, 31] cannot be realized is that the implemented times of such algorithms are longer than T_1 (see the middle and top curves in Figs. 2(a), (c), and (d). Therefore, the algorithms for this number of qubits in Refs. [29, 32] are more efficient than the algorithms in Refs. [28, 30, 31] because of their short realization times. For experiments in the absence of photons, one cannot realize 4-, 5-, ..., N-qubit algorithms in Refs. [29, 32] nor 3-, 4- ..., N-qubit algorithms in Refs. [28, 30, 31] (see Fig. 3).

The resulting calculations showed that the times for implementing the algorithms in Refs. [33, 34] are much less than T_1 and T_2 [see Fig. 2(f)]. Owing to the shortness of these required times, many qubit algorithms in Refs. [33, 34] can be experimentally implemented in the absence of photons in the cavity.

In the presence of photons in the cavity, for example, one or two photons, a sudden shortening of the required times of operation for the above algorithms was observed. This is seen from the results in Figs. 2(a)–(e) and Tables 2 and 3, where, for cavities containing one photon, the implementation times for the two- and three-qubit algorithms in Refs. [28–32] were less than the dephasing times of the systems. Additionally, Figs. 2(a)–(e), show that the required times for four-qubit algorithms in Refs. [29, 32] are less than T_1 while for the algorithms in Refs. [28, 30, 31] these times are greater than T_1.

When the cavity contains two photons, observations proved that the times of implementation for the algorithms in Refs. [28–34] are less than T_1. Consequently, this experimentally confirms the possibility of realizing two-, three-, and four-qubit algorithms [28–32]. Furthermore, when one or two photons exist in the cavity, a significant shortening occurs in the required implementation times of the algorithms mentioned in Refs. [33, 34], and these implementation times are always less than T_1 and T_2 [see Fig. 2(f) and Table 4].

If the number of photons is greater than two in the cavity, the times required by the gates decreases. This,

in turn, decreases the operation times of the algorithms in which they appear. For example, when 40 photons are in the cavity, the times for the algorithms in Refs. [28–32] were 40.7, 20.35, 40.7, 61.04, and 20.35 ns for four qubits. In addition, when $r = 40$ photons, the times of algorithms in Refs. [33, 34] were 20.38, 24.26, and 40.75 as.

Therefore, to realize multi-qubit algorithms, the required times must be less than T_1, because, as the number of photons in the cavity is successively increased, a very significant decrease in the implementation times required for gate operation was observed. Following this reasoning, we see that there was a substantial reduction in the values of the operation times for algorithms implemented based on these types of gates [see Figs. 3(a)–(c)].

In the case of a cavity including 2000 photons [see Figs. 3(a)–(c)], the measured run times of the algorithms were in picoseconds or femtoseconds. These required times for the algorithm operations [28–32] were much less than T_1 and T_2. Therefore, experimentally, when the number of cavity photons is slightly greater than the number of qubits, realization of the N-qubit algorithms can be achieved. Based on the above discussion, one can conclude that the times T_1 and T_2 for $r > N$ did not limit the realization of algorithms composed of N qubits, but the control factor is r. Figure 3(d) shows the realization of a 1000 qubit phase estimation algorithm. The implementation time for the algorithm was the run time required for the operation of a 1000 Hadamard gates, a 1000 $\mathrm{P}_{ee}(\Phi)$ gates, and the operation time of an inverse DQFT. Any of the inverses of the DQFT in Refs. [28–32] can be easily employed. However, we used the inverse of the DQFT in Ref. [28]. The run times of the Hadamard and controlled phase gates were measured in attosecond units, so their run times are very short and almost insignificant when added to the times of the gates that were measured in nanoseconds. Therefore, the behavior of the phase estimated algorithm exactly agreed with that of the behavior of the DQFT in Refs. [28–32]. It should be noted that the discussions represented in Fig. 3(d) are essentially the same as those for Figs. 3(a)–(c).

Therefore, we are in good agreement that the realization times of the quantum gates depend on the number of photons in their cavities (r). Our results showed that the main control in the implementation of any quantum algorithm, whether realized previously or in the future, will require a greater number of photons, r, than the number of qubits, N, i.e., $r > N$. Theoretically, and based on the new technique for the calculating gates, it has been proven that, if gates types with 2, 3, ..., N qubits can be implemented, then these gates can be used in quantum communication, teleportation, and cryptography as well as for the realization of any N-qubit algorithm. The expected required times for implementing the different aspects of quantum computation algorithms when $r > N$ are less than the dephasing and relaxation times, if we assume the ideal case, where the superconducting phase qubits are identical. However, practically, it is hard to achieve two completely identical superconducting phase qubits. In a forthcoming work, we will discuss the effect resulting from this detuning.

6 Conclusion

We presented a novel approximation method for realizing one- and two-qubit gates for the realization of quantum algorithms. As the effect of dephasing and relaxation times can be absorbed into the twisted boundary conditions, we can obtain the exact solution to this system and find the corresponding one- and two-qubit gates. The interplay between interaction and coupling revealed the existence of energy level crossing and ground-state phase transition. The types of required gates to realize N-qubit algorithms and numerical results for the times required for some algorithms were also presented.

Furthermore, future visualizations to implement these algorithms experimentally and the results of the influence of photon number on the required times for their realization were mentioned. However, we concluded that there is no impact of T_1 and T_2 on the realization of quantum algorithms. Hence, we invoked a new approach for quantum algorithm realization. This discussion can be extended further considering the dissipation effect.

Acknowledgements The authors wish to thank Prof. Arthur R. McGurn from Western Michigan University for comments that redressed some of our presentation for this manuscript, we gratefully acknowledge the help provided during the editorial process.

References

1. A. M. Turing, On computable numbers, with an application to the Entscheidungsproblem, *Proc. Lond. Math. Soc.* s2–42(1), 230 (1937)
2. R. P. Feynman, Simulating physics with computers, *Int. J. Theor. Phys.* 21(6–7), 467 (1982)
3. P. Benioff, Quantum mechanical models of Turing machines that dissipate no energy, *Phys. Rev. Lett.* 48(23), 1581 (1982)
4. D. Deutsch, Quantum theory, the Church-Turing Principle and the universal quantum computer, *Proc. R. Soc. Lond. A* 400(1818), 97 (1985)
5. D. Deutsch, Quantum computational networks, *Proc. R. Soc. Lond. A* 425(1868), 73 (1989)
6. D. P. DiVincenzo, Quantum computation, *Science* 270(5234), 255 (1995)

7. D. P. DiVincenzo, The physical implementation of quantum computation, *Fortschr. Phys.* 48(9–11), 771 (2000)
8. M. Nakahara, S. Kanemitsu, M. M. Salomaa, and S. Takagi (Eds.), Physical Realization of Quantum Computing: Are the DiVincenzo Criteria Fulfilled in 2004? Singapore: World Scientific, 2006
9. L. M. K. Vandersypen and I. L. Chuang, NMR techniques for quantum control and computation, *Rev. Mod. Phys.* 76(4), 1037 (2005)
10. E. L. Raab, M. Prentiss, A. Cable, S. Chu, and D. E. Pritchard, Trapping of neutral sodium atoms with radiation pressure, *Phys. Rev. Lett.* 59(23), 2631 (1987)
11. G. Wendin and V. S. Shumeiko, Superconducting quantum circuits, qubits and computing, arXiv: cond-mat/0508729 (2005)
12. B. D. Josephson, Possible new effects in superconductive tunnelling, *Phys. Lett.* 1(7), 251 (1962)
13. B. D. Josephson, The discovery of tunnelling supercurrents, *Rev. Mod. Phys.* 46(2), 251 (1974)
14. U. Meirav, M. A. Kastner, and S. J. Wind, Single-electron charging and periodic conductance resonances in GaAs nanostructures, *Phys. Rev. Lett.* 65(6), 771 (1990)
15. O. Gamel, H. Chan, G. Fleming, and K. B. Whaley, Fully quantum analysis of photosynthetic coherent energy absorption and transfer, *Bull. Am. Phys. Soc.* 62, 4 (2017)
16. B. Schumacher, Quantum coding, *Phys. Rev. A* 51(4), 2738 (1995)
17. J. M. Martinis, Superconducting phase qubits, *Quant. Inf. Proc.* 8(2–3), 81 (2009)
18. H. Eleuch, Entanglement and autocorrelation function in semiconductor microcavities, *Int. J. Mod. Phys. B* 24(29), 5653 (2010)
19. H. Eleuch, Autocorrelation function of microcavity-emitting field in the linear regime, *EPJD* 48(1), 139 (2008)
20. E. A. Sete, A. A. Svidzinsky, H. Eleuch, Z. Yang, R. D. Nevels, and M. O. Scully, Correlated spontaneous emission on the Danube, *J. Mod. Opt.* 57(14–15), 1311 (2010)
21. E. A. Sete, A. A. Svidzinsky, Y. V. Rostovtsev, H. Eleuch, P. K. Jha, S. Suckewer, and M. O. Scully, Using quantum coherence to generate gain in the XUV and X-ray: Gain-Swept superradiance and lasing without inversion, *IEEE J. Sel. Top. Quantum Electron.* 18(1), 541 (2012)
22. H. Eleuch and R. Bennaceur, An optical soliton pair among absorbingthree-level atoms, *J. Opt. A* 5(5), 528 (2003)
23. M. Tinkham, Introduction to Superconductivity, 2nd Ed., New York: McGraw Hill, 1996
24. R. W. Simmonds, K. Lang, D. Hite, S. Nam, D. Pappas, and J. Martinis, Decoherence in Josephson Phase Qubits from Junction Resonators, *Phys. Rev. Lett.* 93(7), 077003 (2004)
25. M. A. Sillanpää, J. I. Park, and R. W. Simmonds, Coherent quantum state storage and transfer between two phase qubits via a resonant cavity, *Nature* **449**, 438 (2007)
26. F. Altomare, J. I. Park, K. Cicak, M. A. Sillanpää, M. S. Allman, D. Li, A. Sirois, J. A. Strong, J. D. Whittaker, and R. W. Simmonds, Tripartite interactions between two phase qubits and a resonant cavity, *Nat. Phys.* 6(10), 777 (2010)
27. O. Gamel and D. F. V. James, Time-averaged quantum dynamics and the validity of the effective Hamiltonian model, *Phys. Rev. A* 82, 052106 (2010)
28. M. A. Nielsen and I. L. Chuang, Quantum Computation and Quantum Information, Cambridge: Cambridge University Press, Ch. 4 and 6 (2000)
29. H. F. Wang, X.Q. Shao, Y.F. Zhao, S. Zhang, and K.H. Yeon, Protocol and quantum circuit for implementing the N-bit discrete quantum Fourier transform in cavity QED, *J. Phys. At. Mol. Opt. Phys.* 43(6), 065503 (2010)
30. H. F. Wang, J. J. Wen, A. D. Zhu, S. Zhang, and K. H. Yeon, Deterministic CNOT gate and entanglement swapping for photonic qubits using a quantum-dot spin in a double-sided optical microcavity, *New J. Phys.* 13, 013021 (2011)
31. H. F. Wang, X. X. Jiang, S. Zhang, and K. H. Yeon, Efficient quantum circuit for implementing discrete quantum Fourier transform in solid-state qubits, *J. Phys. At. Mol. Opt. Phys.* 44(11), 115502 (2011)
32. A. S. F. Obada, H. A. Hessian, A. B. A. Mohamed, and A. H. Homid, Efficient protocol of NN-bit discrete quantum Fourier transform via transmon qubits coupled to a resonator, *Quant. Inf. Proc.* 13(2), 475 (2014)
33. A. H. Homid, A. Abdel-Aty, M. Abdel-Aty, A. Badawi, and A. S. F. Obada, Efficient realization of quantum search algorithm using quantum annealing processor with dissipation, *J. Opt. Soc. Am. B* 32(9), 2025 (2015)
34. D. Deutsch and R. Jozsa, Rapid solution of problems by quantum computation, *Proc. R. Soc. Lond. A* 439(1907), 553 (1992)
35. D. R. Simon, On the power of quantum computation, *Proc. 35th IEEE Symp. Found. Comp. Sci., Santa Fe, NM* 116–123 (1994)
36. D. R. Simon, On the power of quantum computation, *SIAM J. Comput.* 26(5), 1474 (1997)
37. B. C. Sanders and G. J. Milburn, Optimal quantum measurements for phase estimation, *Phys. Rev. Lett.* 75(16), 2944 (1995)
38. P. Shor, Discrete logarithms and factoring, *Proc. 35th Ann. Symp. Found.Comp. Sci.* 124 (1994)

39. P. Shor, Polynomial-time algorithms for prime factorization and discrete logarithms on a quantum computer, *SIAM J. Comput.* 26(5), 1484 (1997)

40. O. Manasreh, Semiconductor Heterojunctions and Nanostructures, New York: McGraw-Hill Profes-sional, 2005

41. R. D. Levine, Quantum Mechanics of Molecular Rate Processes, New York: Dover Publications, 1999

42. N. Froman and P. O. Froman, JWKB Approximation, Amsterdam: North-Holland, Amsterdam, 1965

43. H. Eleuch, Y. V. Rostovtsev, and M. O. Scully, New analytic solution of Schrödinger's equation, *EPL* (*Europhys. Lett.*) 89(5), 50004 (2010)

44. J. Q. You and F. Nori, Superconducting circuits and quantum information, *Phys. Today* 58(11), 42 (2005)